https://doi.org/10.7735/ksmte.2020.29.5.353

J. Korean Soc. Manuf. Technol. Eng.
ISSN 2508-5107(Online)

Finite Element Analysis and Fabrication of an Ultrasonic Milling System

Hyunse Kim[a*], Euisu Lim[a], Kyunghan Kim[a]

[a] *Energy Systems Research Division, Korea Institute of Machinery and Materials*

ARTICLE INFO

Article history:

Received	26	June	2020
Revised	6	August	2020
Accepted	18	August	2020

Keywords:
Ultrasonic
Milling
Finite element method (FEM)
Waveguide
Piezoelectric actuator

ABSTRACT

Ultrasound has been adapted in several industrial and manufacturing applications. In this study, an ultrasonic milling system, which can vibrate a rotating tool, was designed and fabricated. Firstly, a lead zirconate titanate (PZT) was designed using finite element analysis, and the obtained peak impedance value of 47.2 kHz agreed well with the fabricated PZT value of 48.0 kHz. Additionally, an aluminum waveguide with two PZT actuators was analyzed, whose impedance characteristic was predicted to be 43.8 kHz. Consequently, a milling waveguide was fabricated using the analysis results. The impedance value of the fabricated waveguide was measured to be 42.7 kHz, which was consistent with the finite element analysis result with an error of 2.6 %. The rotational speed and power output were measured to be 10,001 rpm and 122.6 W. Thus, the developed milling waveguide can be applied to the milling process of high-hardness metals.

1. Introduction

Until recently, ultrasound has been used in many industrial areas and manufacturing fields. Ultrasound is a wave with a frequency of above 18 kHz, which range is inaudible frequency[1]. It can propagate in solid or liquid medium with different velocity, which mainly depends on the density of the medium. Ultrasound is widely applied in semiconductor cleaning, solar cell cleaning and industrial cleaning processes[2,3]. The cleaning processes are generally performed in liquid status with cleaning chemicals. On the other hand, it can also be applied to metal surface treatment[4]. This process is performed by solid state energy transportation. Luo et al. developed an ultrasonic bonding process for thermoplastic microfluidic devices without energy director[5]. Their bonding process could be done effectively by ultrasound with heat and solvent. In addition, Jang et al. used an ultrasonic metal welder for bonding copper (Cu) sheet[6]. They analyzed Cu sheet deposition characteristics using the ultrasonic metal welder and a tension tester. In a rotary turning process, tool wear is important. So, Lotfi et al. performed research about three-dimensional (3D) finite element simulation of tool wear in ultrasonic assisted rotary turning[7]. They developed a model to predict tool wear and heat distribution on tool faces in an ultrasonic assisted rotary tuning process. There were also research efforts about an ultrasonic burnishing process. Zhou

* Corresponding author. Tel.: +82-42-868-7967
E-mail address: hkim@kimm.re.kr (Hyunse Kim).

et al. reported the wear behavior of aluminum material by ultrasonic-assisted surface burnishing[8]. Teimouri et al. developed an analytical model of the ultrasonic burnishing process, in which the considered parameters were the feed rate, depth of burnishing, ball radius, vibration amplitude, and pass number[9]. Regarding polishing, Zhao et al. researched abrasive polishing (AP) to enhance the surface quality, and to improve machining efficiency[10]. Yu et al. reported experiments about the ultrasonic polishing process to investigate the effect of the ultrasonic vibration field during the process[11]. For grinding applications, Zahedi et al. applied an ultrasonic assisted grinding tool to a grinding process of difficult-to-cut materials[12]. They designed and manufactured the device for utilizing ultrasonic vibrations in external cylindrical grinding. Wen et al. reported the contact performance of an ultrasonic-assisted grinding surface[13]. They found an appropriate ultrasonic amplitude condition to improve the contact performance. Kuo reported design processes of a rotary ultrasonic milling tool using finite element method (FEM) simulation[14]. He performed FEM analysis for designing the milling tool by predicting the amplitude of the system. But he did not explain systematic design processes from a piezoelectric actuator through a whole waveguide with analysis of impedance curves.

There have been many attempts to apply ultrasonic systems, so it is not appropriate to include all the cases in this paper. But a recent paper by Ning et al. seems to properly categorize the ultrasonic applications[15]. In this review paper, ultrasonic vibration-assisted (UV-A) manufacturing processes are analyzed such as turning, forming, and fusion welding. They explain the different underlying mechanisms of ultrasonic vibration actions in a variety of UV-A manufacturing processes. Among the described effectiveness of ultrasound, the general advantage is that it will help to promote chip separation in machining, and reduce the friction or pressure at the interface in mechanical manufacturing processes. We also tried to apply ultrasonic power in the milling process. Although there have been a bunch of researches about ultrasound aided processes, they almost addressed efforts about experiments and analysis of the ultrasonic application processes.

In this research, we designed and fabricated an ultrasonic milling system. In the design process, we used a FEM analysis tool to save development time by trial and error processes. Using the FEM results, a milling waveguide with lead zirconate titanate (PZT) actuators was fabricated. We compared the analysis results with the fabricated waveguide. For power supply, a wireless power transmission module was inserted and assembled. Finally, the rotational speed and power supply were measured for the performance assessment, and the results were discussed.

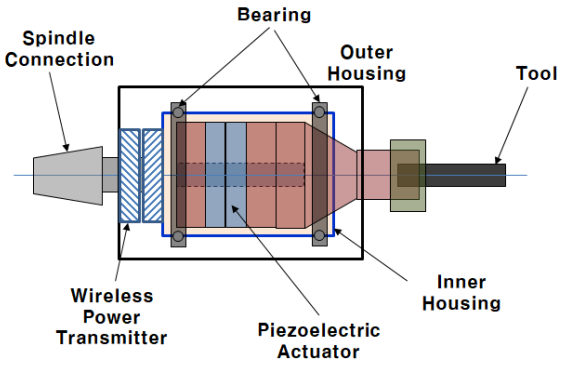

Fig. 1 Inner structure of the ultrasonic milling waveguide

2. Design of an Ultrasonic Waveguide

2.1 Structure and Working Principle

The ultrasonic milling tool is composed of two piezoelectric actuators, a waveguide and a milling tool as shown in Fig. 1. In the case, there are a rotating axis and bearings. The axis is connected to the machine tool for high-speed rotation. The other main component is a power transmission module without brushes, which is a non-contact type. So the first coil is inserted at the top cover part (the left one in Fig. 1, which is indicated as a 'wireless power transmitter'), while the second coil (just beside of the first coil) is placed at the end of the ultrasonic waveguide. Thus, electricity is supplied to the first coil, which then emits a magnetic field to the second coil. The second coil can then obtain induced electricity without contacting the electrode, while maintaining high rotational speed.

The fabricated two milling waveguides are shown in Fig. 2(a), and its assembled view is shown in Fig. 2(b). The material of the waveguide was aluminum (Al) for reducing the weight. Three thin copper electrodes were inserted between the PZTs for supplying electricity. After assembly,

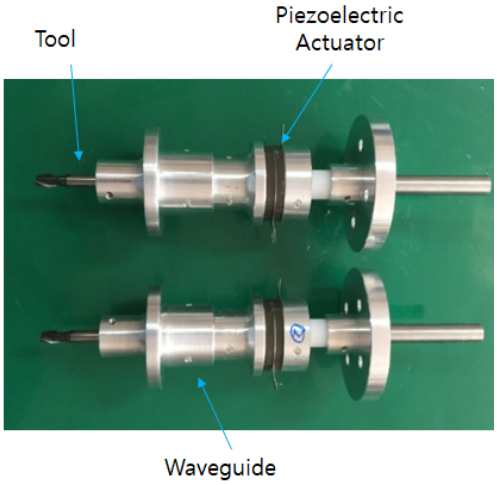

(a) Ultrasonic milling tool

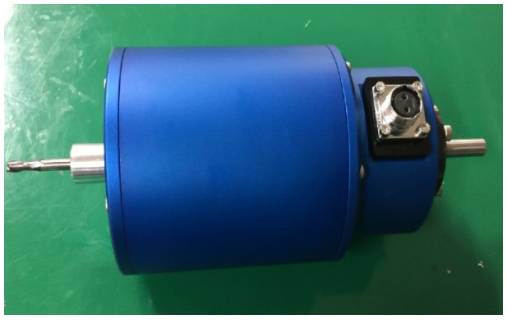

(b) Assembled view

Fig. 2 Fabricated ultrasonic milling tool

key issues were balancing the rotating part for high rotational speed. Precise machining was required for the final assembled product.

When machining with this equipment, it can be installed in conventional machine tool arbors. It is connected by the interface at the end of the waveguide, thus it can obtain rotational motion from the main machine axis. Up to now, it is almost the same as the conventional milling tool cutting. However, different from simple cutting tools, the waveguide is supplied with electric power from the generator up to 100 W for producing longitudinal vibration of 40 kHz frequency. The working principle is illustrated in Fig. 3. General milling process is performed by a cutting tool which is inserted into the machine tool arbor.

When machining high hardness metal, the tool undergoes high resistance by the metal material, which might cause vibration and chattering, and even worse, tool breakage. When introducing ultrasonic vibration to the tool, the resistance is highly reduced, thus smoother cutting can be achieved without

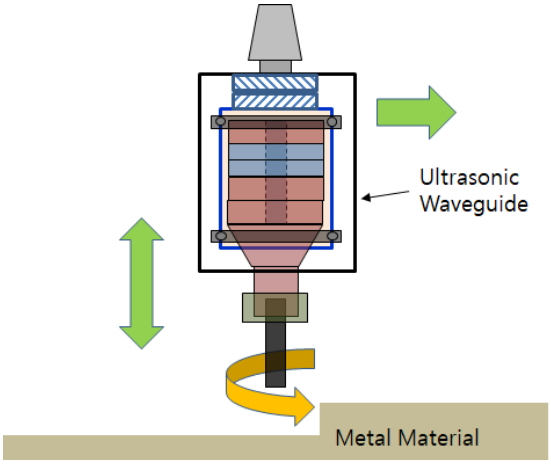

Fig. 3 Working principle of the ultrasonic milling

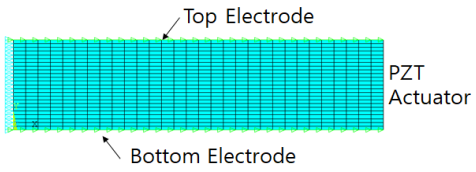

(a) FEM model

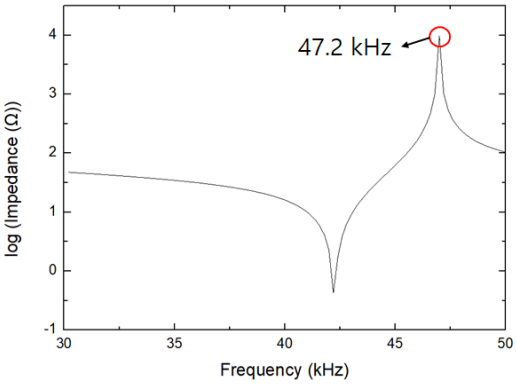

(b) Analysis result

Fig. 4 FEM analysis result of the PZT

tool breakage. This also lengthens the tool life. And it can reduce the machining force through the intermittent cutting phenomenon due to the longitudinal vibration[15]. Sometimes, the cut surface forms micro-texturing, which is effective in reducing the friction coefficient. By regulating the tool path velocity, the texturing roughness can be controlled for certain applications.

2.2 FEM Analysis and Fabrication

In the design process of the ultrasonic milling system, finite element analysis was performed using ANSYS software, which is a commercial FEM tool. To design the waveguide

Table 1 Analysis properties of the PZT actuator

Material	Property	Value
PZT	Stiffness (Nm^{-2})	$\begin{bmatrix} 14.58 & 8.23 & 8.57 & 0 & 0 & 0 \\ & 14.58 & 8.57 & 0 & 0 & 0 \\ & & 13.03 & 0 & 0 & 0 \\ & & & 2.60 & 0 & 0 \\ & \text{Symmetric} & & & 2.60 & 0 \\ & & & & & 3.20 \end{bmatrix}$
	Piezoelectric constants (Cm^{-2})	$\begin{bmatrix} 0 & 0 & 0 & 0 & 13.26 & 0 \\ 0 & 0 & 0 & 13.26 & 0 & 0 \\ -4.24 & -4.24 & 17.28 & 0 & 0 & 0 \end{bmatrix}$
	Dielectric constants [$\varepsilon_s/\varepsilon_0$]	$\begin{bmatrix} 826.20 & 0 & 0 \\ 0 & 826.20 & 0 \\ 0 & 0 & 735.80 \end{bmatrix}$

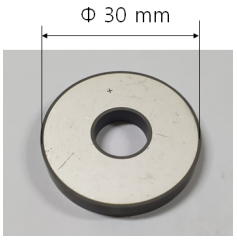

(a) Fabricated PZT

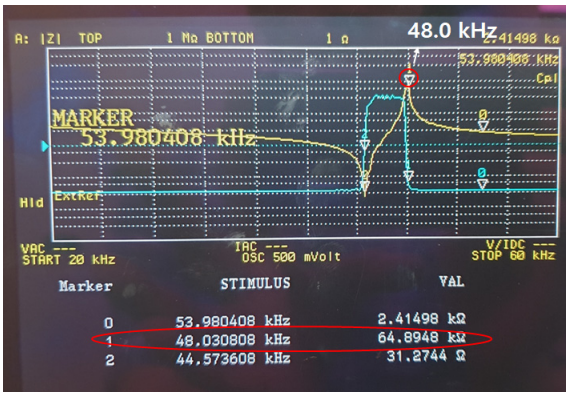

(b) Measured impedance result

Fig. 5 Measured impedance result of the PZT

with PZT actuators, it was modeled two-dimensionally and axis-symmetrically as shown in Fig. 4(a). In the first step, the material of the actuator was given as a PZT, and its property was given to the model. Analysis properties of the PZT actuator are listed in Table 1. We used a 'plane 13' element for the analysis model. To actuate the waveguide, electricity was added as a boundary condition. For this process, the top line and the bottom line were set as electrodes. They were electrically coupled for calculations, and 1 V was given to the top and 0 V to the bottom for grounding the voltage.

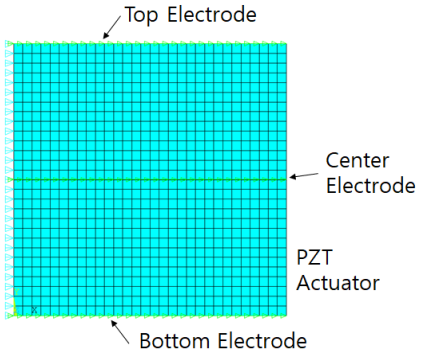

(a) FEM model

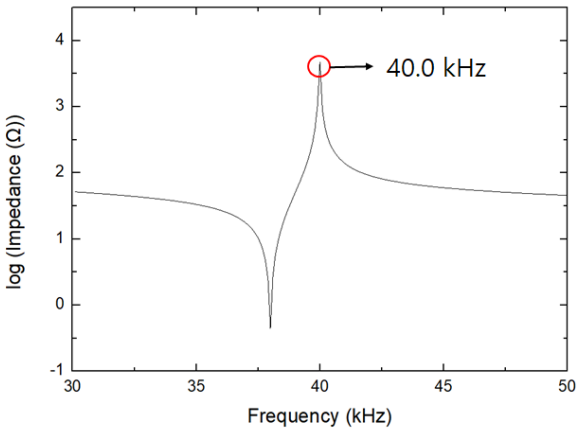

(b) Analysis result

Fig. 6 Analysis result of the two combined PZTs

The calculations were repeated with the same analysis model, while changing the input frequencies from 30.0 kHz to 50.0 kHz. As a result, the impedance graph with a peak frequency value of 47.2 kHz was obtained, as shown in Fig. 4(b). Based on the result, a ring-type PZT actuator was fabricated, which is shown in Fig. 5(a). The frequency of the minimum impedance value could be found just before the peak. At this point, the current through the PZT is high, thus a large amount of heat is generated. So we used the peak point for the design of the system from now on. To verify the analysis, the impedance characteristic of the PZT was also measured to be 48.0 kHz, which agreed well with the peak impedance value of the analysis with 1.7% error, as shown in Fig. 5(b). In the ultrasonic milling system, two PZT actuators are needed to obtain the required power of 100.0 W. Due to a small displacement that is emitted at the end surface of the PZT, we adapted the two ring type PZT actuators, which are combined with a bolt.

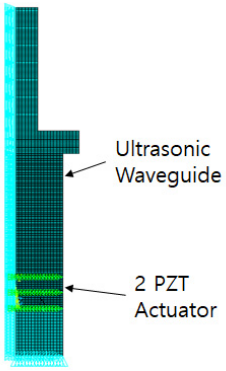

(a) FEM model

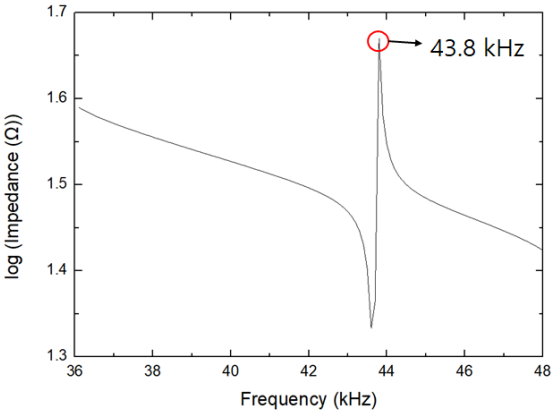

(b) Analysis result

Fig. 7 Analysis result of the milling waveguide with PZT

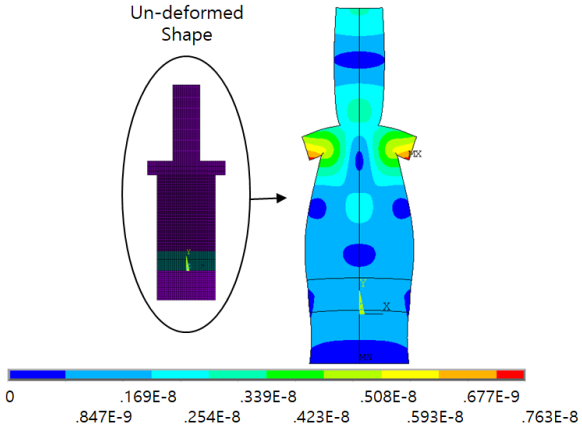

Fig. 8 FEM deformed shape and displacement result

Fig. 9 Experimental impedance result

For analysis, two PZTs were modeled, as shown in Fig. 6(a). Top, center, and bottom electrodes were modeled to divide them. Almost the same procedures were repeated for the modeling process. Impedance analysis was performed between 30.0 kHz and 50.0 kHz. Consequently, the impedance graph showing a peak frequency of 40.0 kHz, was plotted, which is shown in Fig. 6(b). This frequency is set as a design frequency of the system.

Consecutively, a waveguide with the two PZTs were modeled. A waveguide performs the role of amplifying the small displacement from the PZTs. If the area of the first cylindrical Al body that is attached to the PZTs is twice of that of the second body, which is next to the first cylinder, the amplitude is doubled. So, the diameter of the second step was designed to be smaller than the first step. Between the two cylinders, a wing for fixing the body to the case was designed.

We also used the 'plane 13' element for the analysis model of each material. The PZT and the Al model were merged at the interface for the analysis. Almost the same procedures were followed as in the previous analysis. The top and bottom nodes of the two PZTs were given loads of 1 V for the top, and 0 V for the bottom, respectively. The analysis model is shown in Fig. 7(a). The calculation frequency range was from 34.0 kHz to 54.0 kHz. As a result, the peak impedance value of 43.8 kHz was obtained, as shown in Fig. 7(b). Using the frequency value, the deformation and harmonic analysis were done. Larger deformation is observed at the end of the waveguide, as seen in Fig. 8. In addition, the red area indicates large displacement at the frequency.

Reflecting these analysis results, an Al waveguide with two PZT actuators was fabricated, and its characteristic was measured. The result was 42.7 kHz as shown in Fig. 9, which agreed well with the analysis result with error of 2.6%.

And the power transmission module was fabricated as shown in Fig. 10. A couple of power transmission modules were manufactured for the first and the second coil. It is

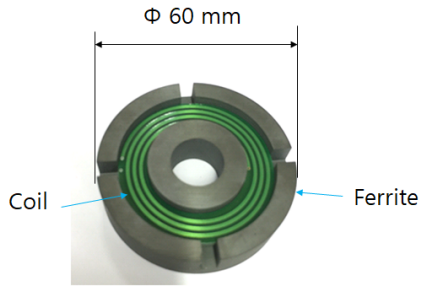

Fig. 10 Fabricated power transmission module

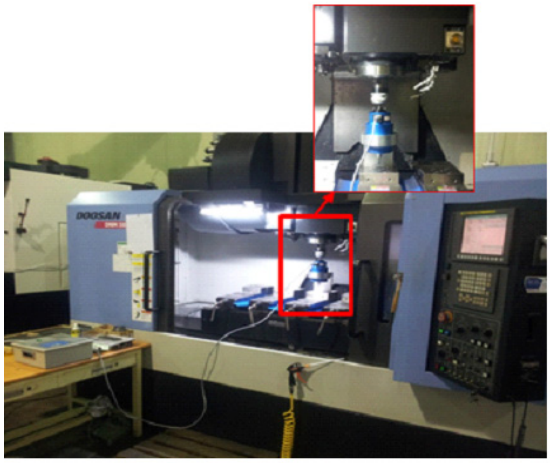

(a) Experimental setup

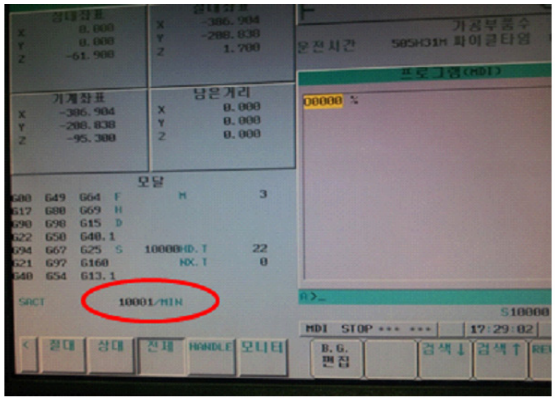

(b) Measured rotational speed

Fig. 11 Rotational speed test result

mainly composed of a ferrite and an electric coil. The diameter of the single module was 60 mm and the thickness was 10 mm.

3. Experiments

Using the fabricated waveguide, the performance test was conducted. First, the rotational speed test was performed, and secondly, the power transmission was measured. To test the

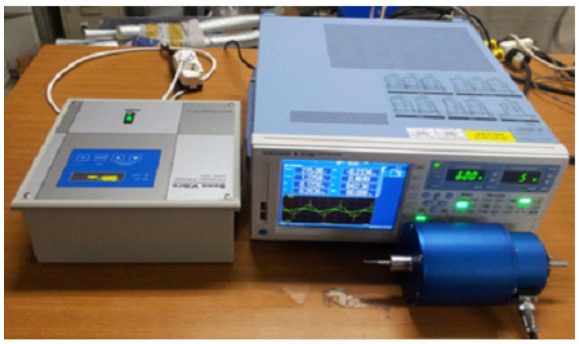

(a) Power measurement setup

(b) Experiment result

Fig. 12 Power measurement experiment result

spindle speed, it was installed in a conventional machine tool, as shown in Fig. 11(a). The obtained rotational speed was 10,001 rpm as shown in Fig. 11(b), while our target value was 10,000 rpm. Then, the power was supplied, and the power transmission was measured. The power measurement setup is shown in Fig. 12(a), and the measured value was 122.6 W, as shown in Fig. 12(b). The measured power satisfied our target value of 100.0 W.

4. Conclusion

In this work, an ultrasonic milling system with an operation frequency of 40 kHz was designed and fabricated. In the design process, finite element analysis was performed for predicting the impedance characteristics of the actuator and the waveguide. First, the ring-type PZT actuator was analyzed, and the obtained peak impedance value was 47.2 kHz. The fabricated PZT was measured to be 48.0 kHz, which agreed well with the peak impedance value of the analysis with 1.7% error. Using this result, two PZTs were modeled and analyzed. The predicted peak impedance value was 40.0

kHz. Referring these results, the whole system of the waveguide with the two PZTs was modeled and analyzed. The calculated peak frequency was 43.8 kHz, which agreed well with the real fabricated Al waveguide characteristic of 42.7 kHz with error of 2.6%. Through the design process using FEM analysis, we could save development time compared to experimental approaches.

In addition, using this system, the rotational speed and the power transmission were measured. As a result, the measured rotational speed was 10,001 rpm, while the power was 122.6 W. The measured rotational speed and power satisfied our target value of 10,000 rpm and 100.0 W, respectively. These results mean that the developed ultrasonic milling system would have the capability to machine process effectively.

Acknowledgment

This research was supported by the Korea Evaluation Institute of Industrial Technology (KEIT), under the Korea government Ministry of Knowledge Economy.

References

[1] Ensminger, D., Bond, L. J., 2012, Ultrasonics: Fundamentals, Technologies and Applications, CRC Press, New York.

[2] Kim, H., Lee, Y., Lim, E., 2015, Dual-frequency Megasonic Waveguide for Nano-pattern Cleaning, IEEE Transactions on Semiconductor Manufacturing, 28:4 521-527, https://doi.org/10.1109/TSM.2015.2469739.

[3] Kim, H., Lim, E., Lee, Y., Park, J.-K., 2019, Fabrication and Performance Tests of an Ultrasonic Cleaning System for Solar-cell Wafers, Journal of The Korean Society of Manufacturing Technology Engineers, 28:4 210-217, https://doi.org/10.7735/ksmte.2019.28.4.210.

[4] Kim, H., Lim, E., Park, J.-K., 2017, Development of a Ultrasonic System for Nano-Surface Reformation Process, Journal of The Korean Society of Manufacturing Technology Engineers, 26:4 365-370, https://doi.org/10.7735/ksmte.2017.26.4.365.

[5] Luo, Y., Zhang, Z., Wang, X., Zheng, Y., 2010, Ultrasonic Bonding for Thermoplastic Microfluidic Devices Without Energy Director, Microelectronic Engineering, 87:11 2429-2436, https://doi.org/10.1016/j.mee.2010.04.020.

[6] Jang, H. S., Park, W. Y., Park D. S., 2011, The Establishment of Bonding Conditions of Cu Using an Ultrasonic Metal Welder, Journal of The Korean Society of Manufacturing Technology Engineers, 20:5 570-575.

[7] Lotfi, M., Amini, S., Aghaei, M., 2018, 3D FEM Simulation of Tool Wear in Ultrasonic Assisted Rotary Turning, Ultrasonics, 88 106-114, https://doi.org/10.1016/j.ultras.2018.03.013.

[8] Zhou, Z.-y., Yu, G.-l., Zheng, Q.-y., Ma, G.-z., Ye, S.-b., Ding, C., Piao, Z.-y., 2020, Wear Behavior of 7075-aluminum After Ultrasonic-assisted Surface Burnishing, Journal of Manufacturing Processes, 51 1-9, https://doi.org/10.1016/j.jmapro.2020.01.026.

[9] Teimouri, R., Amini S., 2019, Analytical Modeling of Ultrasonic Burnishing Process: Evaluation of Active Forces, Measurement, 131 654-663, https://doi.org/10.1016/j.measurement.2018.09.023.

[10] Zhao, Q., Sun, Z., Guo, B., 2016, Material Removal Mechanism in Ultrasonic Vibration Assisted Polishing of Micro Cylindrical Surface on SiC, International Journal of Machine Tools and Manufacture, 103 28-39, https://doi.org/10.1016/j.ijmachtools.2016.01.003.

[11] Yu, T., Guo, X., Wang, Z., Xu, P., Zhao, J., 2019, Effects of the Ultrasonic Vibration Field on Polishing Process of Nickel-based Alloy Inconel718, Journal of Materials Processing Technology, 273 16228, https://doi.org/10.1016/j.jmatprotec.2019.05.009.

[12] Zahedi, A., Tawakoli, T., Akbari, J., 2015, Energy Aspects and Workpiece Surface Characteristics in Ultrasonic-assisted Cylindrical Grinding of Alumina–zirconia Ceramics, International Journal of Machine Tools and Manufacture, 90 16-28, https://doi.org/10.1016/j.ijmachtools.2014.12.002.

[13] Wen, Y., Tang, J., Zhou, W., Zhu, C., 2019, Study on Contact Performance of Ultrasonic-assisted Grinding Surface, Ultrasonics, 91 193-200, https://doi.org/10.1016/j.ultras.2018.08.009.

[14] Kuo, K.-L., 2008, Design of Rotary Ultrasonic Milling Tool Using FEM Simulation, Journal of Materials Processing Technology, 201 48-52, https://doi.org/10.1016/j.jmatprotec.2007.11.289.

[15] Ning, F., Cong, W., 2020, Ultrasonic Vibration-assisted (UV-A) Manufacturing Processes: State of the Art and Future Perspectives, Journal of Manufacturing Processes, 51 174-190, https://doi.org/10.1016/j.jmapro.2020.01.028.

Hyunse Kim

Hyunse Kim is principal researcher in Korea Institute of Machinery and Materials.
His research topics include megasonic cleaning systems for semiconductors, ultrasonic manufacturing processes and ultrasonic cooling.
E-mail: hkim@kimm.re.kr

Euisu Lim

Euisu Lim is principal technician in Korea Institute of Machinery and Materials.
His research topics include megasonic and ultrasonic cleaning systems for semiconductors and flat panel displays (FPD).
E-mail: eslim@kimm.re.kr

Kyunghan Kim

Kyunghan Kim is principal researcher in Korea Institute of Machinery and Materials.
His research interest is laser machining and laser deposition for three-dimensional (3D) printing equipments.
E-mail: khkim@kimm.re.kr